STEM CELLS®

TISSUE-SPECIFIC STEM CELLS

Reactive Oxygen Species Inhibit Adhesion of Mesenchymal Stem Cells Implanted into Ischemic Myocardium via Interference of Focal Adhesion Complex

HEESANG SONG,[a] MIN-JI CHA,[b,c] BYEONG-WOOK SONG,[b,c] IL-KWON KIM,[b,c] WOOCHUL CHANG,[e] SOYEON LIM,[f] EUN JU CHOI,[b,c] ONJU HAM,[b,c] SE-YEON LEE,[b,c] NAMSIK CHUNG,[b,d] YANGSOO JANG,[b,d] KI-CHUL HWANG[b]

[a]Research Institute of Science for Aging, [b]Cardiovascular Research Institute, [c]Brain Korea 21 Project for Medical Science, [d]Cardiology Division, Yonsei University College of Medicine, Seoul, Republic of Korea; [e]Department of Pharmacology, Yale University School of Medicine, New Haven, Connecticut, USA; [f]Cardiovascular Research Institute, University of Rochester School of Medicine and Dentistry, Rochester, New York, USA

Key Words. Mesenchymal stem cells • Transplantation • Reactive oxygen species • Adhesion • Ischemic heart

ABSTRACT

The integrity of transplanted mesenchymal stem cells (MSCs) for cardiac regeneration is dependent on cell–cell or cell–matrix adhesion, which is inhibited by reactive oxygen species (ROS) generated in ischemic surroundings after myocardial infarction. Intracellular ROS play a key role in the regulation of cell adhesion, migration, and proliferation. This study was designed to investigate the role of ROS on MSC adhesion. In H_2O_2 treated MSCs, adhesion and spreading were inhibited and detachment was increased in a dose-dependent manner, and these effects were significantly rescued by co-treatment with the free radical scavenger, *N*-acetyl-L-cysteine (NAC, 1 mM). A similar pattern was observed on plates coated with different matrices such as fibronectin and cardiogel. Hydrogen peroxide treatment resulted in a marked decrease in the level of focal adhesion-related molecules, such as phospho-FAK and p-Src in MSCs. We also observed a significant decrease in the integrin-related adhesion molecules, αV and β1, in H_2O_2 treated MSCs. When injected into infarcted hearts, the adhesion of MSCs co-injected with NAC to the border region was significantly improved. Consequently, we observed that fibrosis and infarct size were reduced in MSC and NAC-injected rat hearts compared to in MSC-only injected hearts. These results indicate that ROS inhibit cellular adhesion of engrafted MSCs and provide evidence that the elimination of ROS might be a novel strategy for improving the survival of engrafted MSCs. STEM CELLS *2010;28:555–563*

Disclosure of potential conflicts of interest is found at the end of this article.

INTRODUCTION

Despite significant advances in the medical management of heart failure, ischemia/reperfusion injury is still a leading cause of death in developed countries [1]. In the last few years, many investigators have shown that mesenchymal stem cell (MSC) transplantation is a promising tool for the repair and regeneration of cardiomyocytes and for the restoration of heart function [2–4]. However, the poor survival of engrafted MSCs is a major obstacle in MSC-based therapy. In fact, several approaches have been developed to enhance grafted cell survival. For example, pretreatment with growth factors, including FGF-2, insulin-like growth factor IGF-1, and BMP-2, has been shown to improve the efficacy of MSC implantation [5]. Also, preconditioning MSCs with hypoxia has been shown to activate the Akt signaling pathway so that cell viability and cell cycle rates are maintained [6]. Genetically modified MSCs that overexpress anti-death signals such as Akt and Bcl-2 also have been shown to be more resistant to apoptosis in vitro and in vivo. The use of these genetically modified MSCs has resulted in dramatic improvement in cardiac function in a rodent myocardial infarction (MI) model, with almost complete replacement of the infarct scar with functioning myocardium [6, 7]. Although prosurvival strategies have proven to be successful in several studies, they do not solve the problems of poor adhesion of MSCs to the cellular matrix. A potentially large contributor to graft cell death in cell-based cardiac repair is anoikis, which is a programmed cell death induced by the loss of matrix attachments [8]. Therefore, enhancement of cell adhesion and spreading should be a major aim in the development of cell transplantation techniques, including the therapeutic use of MSCs.

Author contributions: H.S. and M.-J.C.: manuscript writing, data collection and/or assembly of data, data analysis and interpretation; K.-C.H.: manuscript writing, data collection and/or assembly of data, data analysis and interpretation, provision of study material, data interpretation, conception and design, financial support, final approval of manuscript; B.-W S., I.-K. K., E.J.C., O.H., S.-Y. L.: data collection and/or assembly of data, data analysis and interpretation; W.C., S.L.: provision of study material, data interpretation; N.C., Y.J.: data interpretation, final approval of manuscript.

Correspondence: Ki-Chul Hwang, Ph.D., Cardiovascular Research Institute, Yonsei University College of Medicine, 250 Seongsanno, Seodaemun-gu, Seoul 120-752, Korea. Telephone: 82-2-2228-8523; Fax: 82-2-365-1878; e-mail: kchwang@yuhs.ac Received November 1, 2009; accepted for publication January 4, 2010; first published online in STEM CELLS *EXPRESS* January 13, 2010. 1066-5099/2009/$30.00/0 doi: 10.1002/stem.302

Once MSCs are injected into the infarcted region, they initially encounter harsh conditions coupled with the loss of survival signals because of inadequate interactions between the cells and the matrix [9]. Reactive oxygen species (ROS) may intensify anoikis signals in transplanted MSCs at the infarcted area. In fact, it has been reported that the generation of ROS is dramatically increased over three-fold in the risk region in ischemia/reperfusion-injured animal hearts compared to wild-type animal hearts [10, 11] even though ROS are formed as a natural component of oxygen respiration [12]. Moreover, recent evidence suggests that disruption of integrin contacts in fibroblasts can lead to cell detachment that is preceded by a rise in intracellular ROS levels [13]. Reactive oxygen species can also induce an inflammatory response as well as hinder cell adhesion, leading to cell death [14]. However, the role of ROS in implanted stem cell adhesion in infarcted hearts has not been studied.

In this study, we showed that ROS hinder MSC adhesion to various kinds of matrices and that the elimination of ROS in the transplanted region of an infarcted heart can enhance the adhesiveness of MSCs, leading to greater beneficial effects in cardiac repair.

Materials and Methods

Reagents

Dulbecco's modified Eagle's medium (DMEM), fetal bovine serum (FBS), and penicillin–streptomycin were obtained from Gibco BRL (Grand Island, NY, http://www.invitrogen.com). Focal adhesion kinases (FAK) and phospho-FAK antibodies were purchased from Santa Cruz Biotechnology (Santa Cruz, CA, http://www.scbt.com). Vinculin, paxillin, Rac1, and p-Src antibodies were from Chemicon (Chemicon International Inc., Temecula, CA, http://www.chemicon.com). Horseradish peroxidase-conjugated secondary antibodies to mouse or rabbit were obtained from Santa Cruz Biotechnology. The Western blotting detection system was from Amersham Biosciences (Amersham Pharmacia Biotech, Tokyo, Japan, http://www1.gelifesciences.com). For polymerase chain reaction (PCR), the oligonucleotides synthesized from Bioneer (Bioneer Corporation, Daejeon, Korea, http://www.bioneer.co.kr) and RT-&GO were used for reverse transcription and cDNA synthesis (MP Biomedicals, Solon, OH, http://www.mpbio.com). *N*-acetyl-L-cysteine (NAC) was purchased from Sigma (Sigma, St. Louis, MO, http://www.sigma.com).

Isolation and Culture of MSCs

Mesenchymal stem cells were purified as previously described [2]. Briefly, bone marrow from femoral and tibial bones of four-week-old male Sprague-Dawley rats (approximately 100 g) was aspirated with 10 ml of Dulbecco's modified Eagle's medium (DMEM) supplemented with 10% fetal bovine serum and 1% antibiotic-penicillin/streptomycin solution. Mononuclear cells recovered after centrifugation in Percoll were washed twice, resuspended in 10% FBS–DMEM, and plated in flasks at 1×10^6 cells per 100 cm^2. Cultures were maintained at 37°C in a humidified atmosphere containing 5% CO_2. After 48 or 72 hours, nonadherent cells were discarded, and adherent cells were thoroughly washed twice with phosphate-buffered saline (PBS). Fresh complete medium was added and replaced every 3-4 days for approximately 10 days. For further purification, the Isolex Magnetic Cell Selection System (Baxter Healthcare Corporation, Irvine, CA, http://www.baxter.com) was used. Briefly, cells were incubated with Dynabeads M-450 coated with anti-CD34 monoclonal antibody. A magnetic field was applied, and CD34+ cell-bead complexes were separated from the remaining cell suspension; the CD34− fraction was then cultured. Cells were harvested after incubation with 0.25% trypsin and 1 mM EDTA for 5 minutes at 37°C, replated in 1×10^5 per 100 cm^2 plates, and grown for approximately 10 days. The characteristics of MSCs were demonstrated by immunophenotyping. To verify the nature of cultured MSCs, cells were labeled against various surface and intracellular markers and analyzed by flow cytometry. Cells were harvested, washed with PBS, and labeled with the following antibodies conjugated with fluorescein isothiocyanate (FITC) or Texas red: CD14, CD34, CD71, CD90, CD105, CD106, and ICAM-1. FITC-conjugated goat anti-mouse IgG and Texas red-conjugated goat anti-rabbit IgG from Jackson ImmunoResearch Laboratories (West Grove, PA, http://www.jacksonimmuno.com) were used as secondary antibodies. Labeled cells were assayed by flow cytometry and analyzed with CellQuest Pro Software (Becton-Dickinson, San Jose, CA, http://www.bd.com).

Assays for Cell Adhesion and Spreading

Suspensions of 2×10^4 viable MSCs were added to each well of a four-well plate and allowed to attach for 1 hour at 37°C and 5% CO_2. Hydrogen peroxide was used as the exogenous ROS source, and NAC was used as an ROS scavenger. To determine MSC adhesion, plates were carefully washed three times with PBS, and then four separate fields were photographed with a phase-contrast microscope and counted. Each experiment was performed in triplicate wells and repeated at least three times. For spreading assays, MSCs were plated for 4 hours on four-well plates using the conditions of the adhesion experiments described above. To determine MSC spreading, plates were washed three times with PBS, fixed with 3% formaldehyde, stained with Coomassie blue, and destained, and then four separate fields were photographed using a phase-contrast microscope.

Measurement of Intracellular ROS

Intracellular ROS were measured using a fluorescent dye technique. Cells cultured on glass cover slips were treated for 10 minutes with 10 μM 2′,7′-dichlorofluorescin diacetate (H_2DCFDA; Molecular Probes Inc., Eugene, OR, http://probes.invitrogen.com) in PBS. The probe H_2DCFDA (10 μM) entered into the cells, and the acetate groups on the H_2DCFDAs were cleaved by cellular esterases, trapping the nonfluorescent 2′,7′-dichlorofluorescin (DCFH) within the cells. Subsequent oxidation by reactive oxygen species yielded the fluorescent product DCF. The coverslips were placed in the chamber, which was mounted on the stage of an inverted microscope (Axiovert; Carl Zeiss, Germany, http://www.zeiss.com) equipped with a confocal laser-scanning system (Oz; Noran Instruments, Middleton, WI, http://www.thermo.com). The dye, when exposed to an excitation wavelength of 480 nm, emitted light at 535 nm only when it had been oxidized. Labeled cells were examined for the oxidized dye using a luminescence spectrophotometer. Fluorescence images were collected using a confocal microscope (Leica, Solms, Germany, http://www.leica.com) by excitation at 488 nm and emission greater than 500 nm with a long-pass barrier filter.

Reverse Transcription PCR Analysis

The expression levels of the various genes were analyzed by reverse transcription polymerase chain reaction (RT-PCR). Total RNA was prepared using the Ultraspect-II RNA system (Biotecx Laboratories Inc., Houston, TX, http://www.biotecx.com), and single-stranded cDNA was then synthesized from the isolated total RNA by Avian Myeloblastosis virus (AMV) reverse transcriptase. A 20 μl reverse transcription reaction mixture containing 1 μg of total RNA, 1× reverse transcription buffer (10 mM Tris-HCl, pH 9.0, 50 mM KCl, 0.1% Triton X-100), 1 mM deoxynucleoside triphosphates, 0.5 unit of RNase inhibitor, 50 pmol of oligo$(dT)_{15}$, and 15 units of AMV reverse transcriptase was incubated at 42°C for 15 minutes, heated to 99°C for 5 minutes, and then incubated at 4°C for 5 minutes. Polymerase chain reaction was performed for 35 cycles with 3′ and 5′ primers based on the sequences of the various genes. Glyceraldehyde 3-phosphate

dehydrogenase (GAPDH) (5′-CTCCCAACGTGTCTGTTGTG-3′ and 5′- TGAGCTTGACAAAGTGGTCG-3′) was used as an internal standard. The signal intensity of the amplification product was normalized to its respective GAPDH signal intensity.

Immunoblot Analysis

Cells were washed once in PBS and lysed in buffer (Cell Signaling Technology, Beverly, MA, http://www.cellsignal.com) containing 20 mM Tris (pH 7.5), 150 mM NaCl, 1 mM Na_2-EDTA, 1 mM EGTA, 1% Triton, 2.5 mM sodium pyrophosphate, 1 mM β-glycerophosphate, 1 mM Na_3VO_4, 1 mg/ml of leupeptin, and 1 mM phenylmethylsulfonyl fluoride. Protein concentrations were determined using the Bradford Protein Assay Kit (Bio-Rad, Hercules, CA, http://www.bio-rad.com). Proteins were separated in a 12% sodium dodecyl sulfate–polyacrylamide gel and transferred to a polyvinylidene difluoride membrane (Chemicon International Inc.). After membrane blocking with Tris-buffered saline–Tween 20 (TBS-T, 0.1% Tween 20) containing 5% nonfat dried milk for 1 hour at room temperature, the membrane was washed twice with TBS-T and incubated with primary antibody for 1 hour at room temperature or overnight at 4°C. The membrane was washed three times with TBS-T for 10 minutes and incubated for 1 hour at room temperature with horseradish peroxidase-conjugated secondary antibodies. After extensive washing, bands were detected by enhanced chemiluminescence reagent (Santa Cruz Biotechnology). Band intensities were quantified using the Photo-Image System (GE life sciences).

Immunocytochemistry

Cells were grown on four-well plastic dishes, washed twice with PBS, and then fixed with 4% paraformaldehyde in 0.5 ml of PBS for 30 minutes at room temperature. The cells were washed again with PBS and then permeabilized for 30 minutes in PBS containing 0.2% Triton. Next, the cells were blocked in PBS containing 10% goat serum and incubated for 1 hour with primary antibodies including αV, Fn, p-FAK, p-Src, Rac1, paxillin, and vinculin. The cells were washed again three times for 10 minutes with PBS and incubated with Fluorescein isothiocyanate (FITC)-conjugated goat anti-rabbit IgG and Texas red-conjugated goat anti-mouse IgG (Jackson ImmunoResearch, West Grove, PA, http://www.jacksonimmuno.com) as secondary antibodies for 1 hour. All images were produced using an excitation filter under reflected light fluorescence microscopy and transferred to a computer equipped with MetaMorph software ver. 4.6 (Universal Imaging Corp., Marlow, U.K., http://www.universal-imaging.co.uk).

Induction of Myocardial Infarction

Experiments were conducted in accordance with the International Guide for the Care and Use of Laboratory Animals. The protocol was approved by the Animal Research Committee of the Yonsei University College of Medicine. Under general anesthesia, eight-week-old Sprague-Dawley male rats (about 250 g) were intubated, and positive-pressure ventilation (180 ml/minute) was maintained with room air supplemented with oxygen (2 l/minute) using a Harvard ventilator. The heart was exposed through a 2-cm left lateral thoracotomy. The pericardium was incised and a 6-0 silk suture (Johnson & Johnson, Belgium, http://www.jnj.com) was placed around the proximal portion of the left coronary artery, beneath the left atrial appendage. Ligature ends were passed through a small length of plastic tube to form a snare. For coronary artery occlusion, the snare was pressed onto the surface of the heart directly above the coronary artery, and a hemostat was applied to the snare. Ischemia was confirmed by the blanching of the myocardium and dyskinesis of the ischemic region. After 60 minutes of occlusion, the hemostat was removed and the snare was released for reperfusion, with the ligature left loose on the surface of the heart. Restoration of normal rubor indicated successful reperfusion. Wounds were sutured, and the thorax was closed under negative pressure. Rats were weaned from mechanical ventilation and returned to cages to recover. In sham-operated rats, the same procedure was executed without tightening the snare.

MSC Labeling and Transplantation

Mesenchymal stem cells were labeled with 4′,6-diamidino-2-phenylindole (DAPI) to determine cell viability by adding sterile DAPI solution to the culture medium for 10 minutes on the day of implantation, at a final concentration of 50 μg/ml. Cells were rinsed six times in PBS to remove unbound DAPI. Labeled cells were trypsinized and suspended in serum-free medium for grafting. For instant transplantation after surgical occlusion of the left anterior descending coronary artery, MSCs (2×10^5 cells) were suspended in 10 μl of serum-free medium with or without NAC (1 mM final concentration) and kept on ice until injection with a 30-gauge needle on a Hamilton syringe at three sites, into the anterior and lateral aspects of the viable myocardium bordering the infarction. There were four groups of eight rats each used in this study: (1) normal, (2) NAC control, (3) MSCs control, and (4) NAC and MSCs-implanted.

Histology and Determination of Myocardial Infarct Size and Surviving Cells

Transplanted animals were euthanized at three days after implantation and their hearts were excised, perfusion-fixed with 10% (v/v) neutral-buffered formaldehyde for 24 hours, transversely sectioned into four comparable sections, and embedded in paraffin using routine methods. The 2-μm sections were mounted onto gelatin-coated glass slides to allow for the use of different stains on successive sections of tissue cut through the implantation area. After deparaffinization and rehydration, the sections were stained with hematoxylin and eosin to assess nuclei, cytoplasm, and connective tissue. Histological analyses were performed using the manufacturer's instructions (Vector Laboratories, Burlingame, CA, http://www.vectorlabs.com). 2,3,5-Triphenyltetrazolium chloride (TTC) staining was used to assess myocardial tissue viability and to determine the size of the myocardial infarct. The tissue slices were incubated in a 1% TTC (Sigma) solution, pH 7.4, at 37°C for 20 minutes. The tissues were fixed in 10% PBS buffered formalin overnight at 2-8°C. The hearts were sectioned transaxially, and the size of myocardial infarction was evaluated as a percentage of the sectional area of the infarcted tissue of the left ventricle to the sectional area of the whole left ventricle. Both sides of each TTC-stained tissue slice were photographed with a digital camera. To evaluate the number of surviving cells, we photographed four separate fields by fluorescent microscope and then counted the DAPI-labeled cells. All histological data in this study was treated and analyzed by three persons blinded.

Terminal Deoxynucleotidyl Transferase-Mediated dUTP Nick-End Labeling Assay

The transferase-mediated dUTP nick-end labeling (TUNEL) assay was performed according to the manufacturer's instructions (Chemicon International Inc.). In brief, excised heart tissues were fixed in 3.7% buffered formaldehyde and embedded in paraffin. Five-micrometer-thick tissue sections were deparaffinized, rehydrated, and rinsed with PBS. A positive control sample was prepared from normal heart treated with DNase I (10 U/ml, 10 minutes at room temperature). Sections were pretreated with 3.0% H_2O_2, subjected to TdT enzyme reaction at 37°C for 1 hour, and incubated with digoxigenin-conjugated nucleotide substrate at 37°C for 30 minutes. Nuclei exhibiting DNA fragmentation were stained with 3,3-diaminobenzidine (DAB) (Vector Laboratories) for 5 minutes. Apoptotic cardiomyocytes nuclei were stained dark brown. Lastly, sections were counterstained with methyl green and covered with coverslips. Sections were observed by light microscopy; six slices per group were prepared, with ten regions observed on each slice (×400).

Determination of Microvessel Density

Histological analyses were performed according to the manufacturer's instructions (R.T.U VECTASTAIN Universal Quick Kit; Vector Laboratories). In brief, the excised heart tissues were fixed

in 3.7% buffered formaldehyde and embedded in paraffin. Tissue sections, 5-μm thick, were deparaffinized, rehydrated, and rinsed with PBS. Antigen retrieval was performed with 10 mM sodium citrate (pH 6.0) in a microwave for 10 minutes. Sections were incubated in 3% H_2O_2 to quench the endogenous peroxidase. The samples were blocked in 2.5% normal horse serum and incubated with anti-CD31 antibodies. Biotinylated pan-specific universal secondary antibody 1,360 ILK and streptavidin/peroxidase complex reagent were used to treat the heart sections. Using the DAB substrate kit, the heart sections were stained with antibodies. Counterstaining was performed with 1% methyl green and dehydration was conducted with 100% *N*-butanol, ethanol, and xylene before mounting in VectaMount Mounting Medium (Vector Laboratories). For quantification, capillaries were counted in ten randomly chosen fields from two separate slides at 20×. The mean number of capillaries per field in the infarcted myocardium was used for statistical analysis.

Statistical Analysis

All quantified data represent an average of at least triplicate samples. The error bars represent the standard deviation of the mean. Statistical significance was determined by Student's *t*-test, with $p < .05$ considered significant.

Results

Scavenging ROS by NAC Rescues the Impaired MSC Adhesion and Spreading Induced by Exogenous H_2O_2

MSCs were isolated from mixed culture with hematopoietic cells based on their attachment to the culture plate and further purified by exclusion with magnetic beads targeting the hematopoietic marker CD34. Yield was 3×10^6 cells (95% purity) after 2 weeks of culture. Consistent with a previous report [15, 16], the cultured MSCs expressed CD71, CD90, CD105, CD106, and ICAM-1, but not the hematopoietic and macrophage markers, CD34 and CD14, respectively (data not shown).

To determine whether ROS inhibit MSC adhesion, we performed quantitative adhesion assays with MSCs treated exogenously with H_2O_2. As seen in Figure 1A, the inhibition of MSC adhesion on cultured plastic surfaces was triggered at an H_2O_2 concentration of 20 μM and gradually increased in a dose-dependent manner. We observed that the survival and proliferative activity of MSCs were inhibited starting at a H_2O_2 concentration of 50 μM (supporting information Fig. 1A), indicating that 20 μM H_2O_2 is a sufficiently sublethal level in terms of inducing the loss of cell–matrix adhesion of MSC.

To confirm that the effects of exogenous H_2O_2 on the decrease in MSCs adhesion were specifically due to ROS, we investigated the effects of the ROS scavenger, NAC, on the adhesion of H_2O_2-treated MSCs. First, we confirmed the ROS scavenging effects of NAC using fluorescence to measure intracellular ROS. We observed that the level of intracellular ROS markedly increased by ~two-fold after treatment with 20 μM H_2O_2, and this increase in ROS was inhibited by treatment with 1 mM NAC (Fig. 1B). We conducted studies using different concentrations of NAC to examine potential cell apoptosis. We observed that 1 mM NAC did not induce any damage or apoptosis to the cells (data not shown). Therefore, 1 mM NAC was chosen to conduct the following experiments. The H_2O_2-induced reduction in MSC adhesion was significantly restored by NAC treatment (Fig. 1C). These results indicate that ROS inhibits MSC adhesion to the matrix, and this decrease in MSC adhesiveness can be recovered by the elimination of ROS.

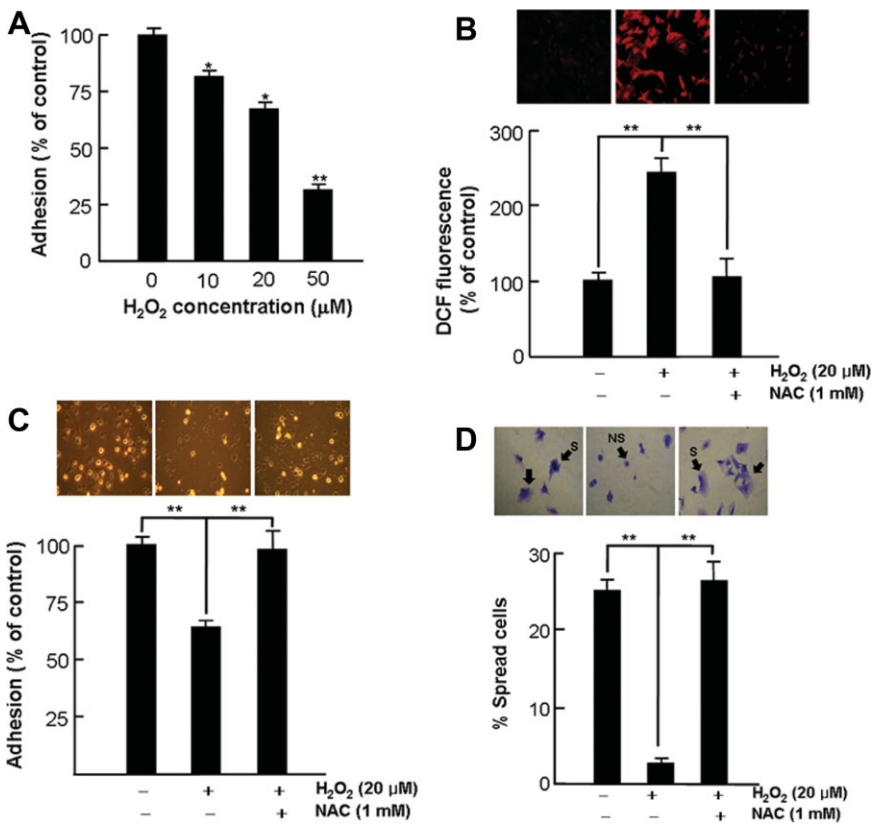

Figure 1. The anti-oxidant, NAC, restores reactive oxygen species (ROS)-induced impairment of mesenchymal stem cell (MSC) adhesion and spreading. **(A):** The effects of exogenous ROS and H_2O_2 on MSC adhesion. Adhesive differences of MSCs in the presence of various concentrations of H_2O_2 were evaluated 1 hour after plating. **(B):** Scavenging intracellular ROS by anti-oxidant, NAC. MSCs were treated with H_2O_2 with or without NAC and then intracellular ROS were measured using H_2DCFDA reagent as described in the Materials and Methods section. Cell images were obtained with a confocal laser microscope. **(C):** The effects of scavenging ROS and NAC on MSC adhesion in the presence of H_2O_2. **(D):** The effects of exogenous ROS and H_2O_2 on MSC spreading with and without NAC. Values are the average of three measurements with the S.D. indicated by error bars (*, $p < .05$, **, $p < .01$). Abbreviations: NAC, *N*-acetyl-L-cysteine.

To further confirm the effects of ROS on MSC adhesion and survival, we performed spreading and trypsinization assays with H_2O_2-treated MSCs. Because spreading is required for the survival of attached cells [17], the absence of spreading will result in cell death. The spreading of cells was drastically decreased in H_2O_2-treated MSC cultures compared to control MSC cultures at the indicated time (typically 12.5% of control values). We observed that this decrease in spreading after H_2O_2 treatment was reversed by NAC pretreatment up to the control level (Fig. 1D). We further examined the adhesion of MSCs on different matrices, such as Fn and cardiogel, as Fn is well known to act as a receptor for integrin-related cell adhesion [18]. Furthermore, cardiogel, a three-dimensional matrix derived from cardiac fibroblasts, has more biological activities relevant to living organisms in comparison to those with 2D matrices. These distinctive in vivo 3D matrix adhesions differ in structure, localization, and function from classically described in vitro adhesions [19]. Although the cell adhesions to both the Fn-coated plates and the cardiogel were significantly increased as compared with adhesion to bare plates, H_2O_2 treatment significantly reduced the amount of adhered MSCs at the indicated times, regardless of the coating material (supporting information Fig. 1B). As expected, NAC treatment successfully restored MSC adhesion to the control level. We also observed a similar pattern in a trypsinization assay, where more cells were easily detached by 0.025% trypsin from H_2O_2-treated MSCs cultures than from control cultures, and the detachment was prevented by NAC, as shown in supporting information Figure 1C.

ROS Downregulates Adhesion-Related Molecules in MSCs

Since it is well established that cell adhesion is mediated mainly by integrin $\alpha V\beta 3$ and the $\beta 1$ family integrin $\alpha 5\beta 1$ [20], we evaluated the altered expressions of adhesion-related integrin molecules in H_2O_2-treated MSCs using RT-PCR. As shown in Figure 2A, the mRNA level of $\beta 1$ was dramatically decreased by ~90% in H_2O_2-treated MSCs compared to in control MSCs. Although this decrease was significantly rescued by NAC, the level was still 60% that of the control MSCs. In the case of αV, the mRNA level was also significantly decreased by ~60% in H_2O_2-treated MSCs compared to control MSCs, and the reduced mRNA levels were also partially rescued by NAC treatment (Fig. 2B). These results indicate that integrin molecules might partly contribute to the ROS-induced loss of MSC adhesion, to which other molecules or mechanisms may be associated.

Integrin is known to activate the cellular focal adhesion-related kinases FAK and Src at the adhesive stage [21]. In addition, activated integrins bind to the extracellular matrix to initiate focal adhesions by recruiting cytoplasmic proteins, such as FAK, Src, and paxillin, which act as linkers between integrins and the actin cytoskeleton [22]. Therefore, we investigated the effects of the above-mentioned proteins at the early adhesive stage. Hydrogen peroxide treatment significantly decreased the phosphorylation of both kinases, FAK and Src, by ~70% compared to that for the control MSCs, which were rescued by NAC treatment. The rescued phosphorylation levels returned to 70% and 90% of initial, respectively, in p-FAK and p-Src of control MSCs (Fig. 2C and 2D). Interestingly, there was a slight, but significant, decrease in the expression levels of vinculin and paxillin, which were rescued by NAC treatment (supporting information Fig. 2A and 2B). We also observed that the level of Rac-1, a small GTPase that is required for cell adhesion and spreading [23], was significantly decreased in H_2O_2-treated MSCs compared to control MSCs (Fig. 2E). These results indicate that ROS hinders MSC adhesion through downregulating integrin-dependent adhesion molecules.

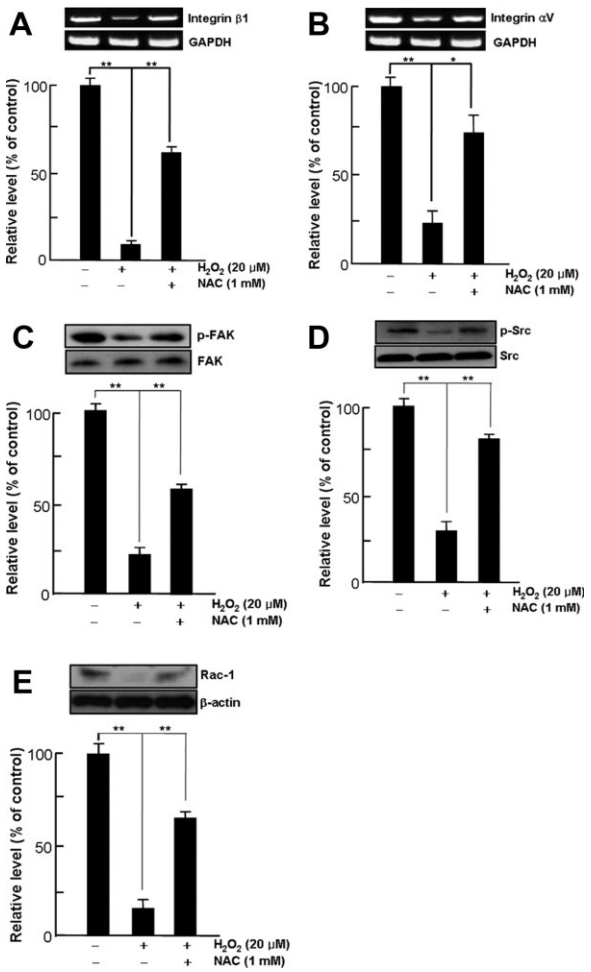

Figure 2. Reactive oxygen species downregulates integrin-related focal adhesion proteins. The mRNA levels of integrin molecules **(A)** integrin b1 and **(B)** integrin αV in H_2O_2-treated mesenchymal stem cells with/without NAC were analyzed by reverse transcription polymerase chain reaction, and the expression levels of focal adhesion-related kinases such as **(C)** p-FAK, **(D)** Src kinase, and **(E)** Rac-1 were analyzed by Western blot. Cells were incubated for 2 hours under designated conditions and then analyzed. Densitometric analysis of three independent triplicate Western blots. Values are the average of three measurements with the S.D. indicated by error bars (*, $p < .05$, **, $p < .01$). Abbreviations: FAK, focal adhesion kinases; GAPDH, glyceraldehyde 3-phosphate dehydrogenase; NAC, *N*-acetyl-L-cysteine.

ROS Impairs the Distribution and Localization of Focal Adhesion Proteins in MSCs

Since FAK and Src-dependent integrin signaling events culminate in reorganization of the actin cytoskeleton, which is a prerequisite for changes in cell shape, adhesion, and gene expression, we investigated the distribution and localization of focal adhesion proteins in H_2O_2-treated MSCs. We first observed that the cells treated with H_2O_2 were round and brilliant and did not show any cytoskeletal organization, whereas the control and H_2O_2-treated cells in the presence of NAC displayed a tightly adhesive and widened morphology with membrane ruffles, which began to extend filopodia around 3 hours after adhesion (Fig. 3). Furthermore, double-immunostaining showed that integrin $\beta 1$ and p-FAK were colocalized

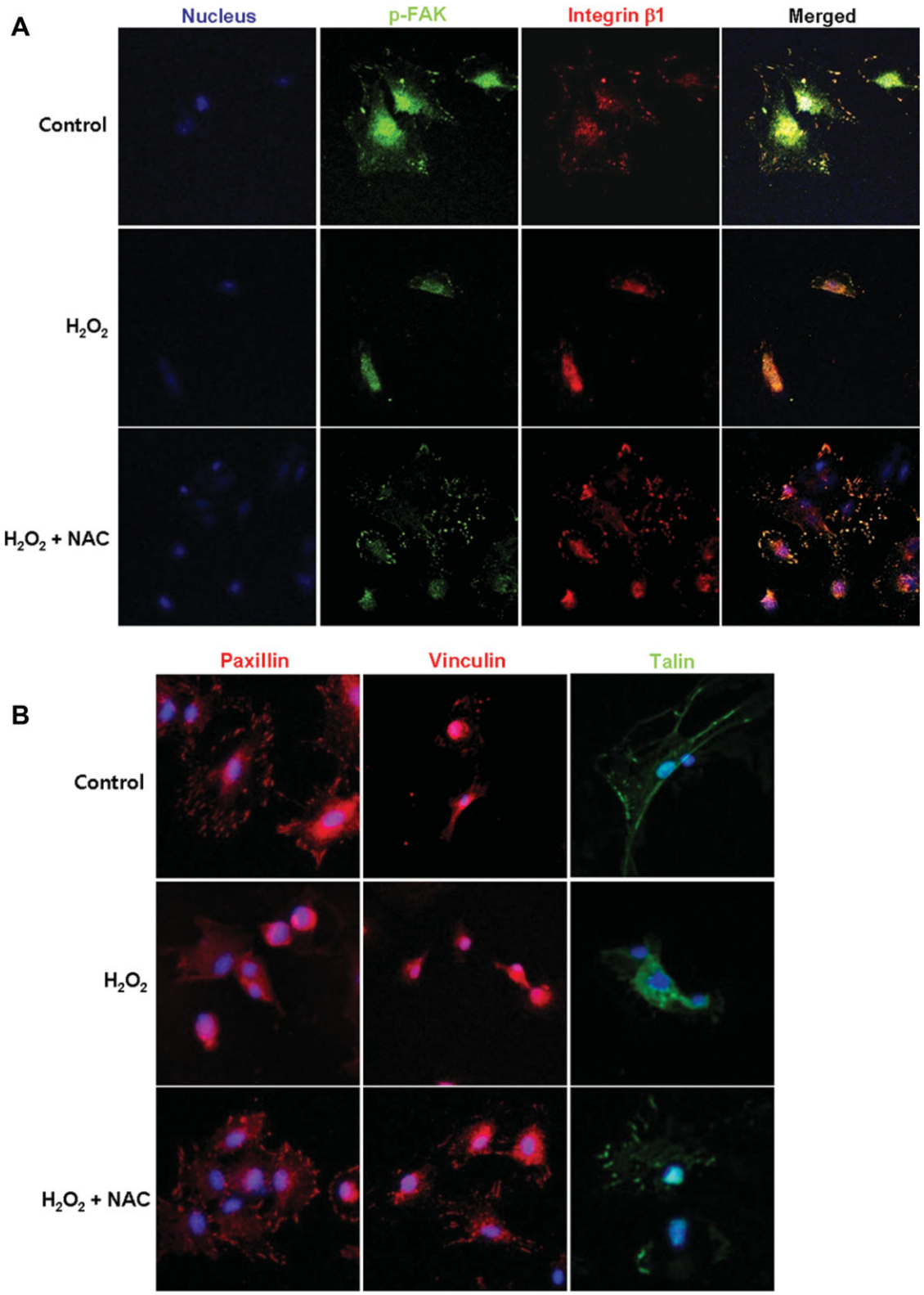

Figure 3. Reactive oxygen species disrupt the localization of integrin-related focal adhesion proteins. **(A):** Double immunostaining for integrin $\beta 1$ and p-FAK. **(B):** Immunostaining for focal adhesion proteins such a, paxillin, vinculin, and talin. Cells were incubated for 2 hours under the designated conditions and then immunofluor-stained. Representative images are shown. Abbreviations: FAK, focal adhesion kinases; NAC, *N*-acetyl-L-cysteine.

at the site of filopodia growth in both the control and H_2O_2-treated MSCs in the presence of NAC. This colocalization suggests that integrin molecules are involved in focal adhesion formation and cytoskeletal organization in MSCs (Fig. 3A). In addition, we did not observe any specific staining for focal adhesion proteins such as paxillin, vinculin, or talin in the H_2O_2-treated MSCs, whereas both the control and H_2O_2-treated cells in the presence of NAC produced numerous peripherally

distributed proteins at the site of the prominent membrane ruffles (Fig. 3B). Our results clearly indicate that ROS impairs MSC adhesion through the disruption of integrin-related focal adhesion, which can be rescued by treatment with antioxidants such as NAC.

Scavenging ROS Enhances the Adhesion of Engrafted MSCs and Improves Myocardial Repair

To investigate whether scavenging ROS facilitated the adhesion of implanted MSCs, we transplanted MSCs labeled with DAPI with/without NAC into the border region between the infarcted and normal areas of the heart after coronary ligation. After three days, the hearts were removed and the fate of the MSCs was investigated using confocal microscopy. A higher number of MSCs coupled with NAC were retained in the border region than in the control MSCs (MSCs-NAC vs. MSCs: 722 ± 55 vs. 263 ± 48, respectively, $p < .001$) (Fig. 4A). In addition, time course experiments indicated enhanced survival of MSCs in the presence of NAC compared to MSCs in the absence of NAC (data not shown). One week after coronary ligation, the size of the left ventricular infarct was evaluated in both the transplanted and control groups using TTC staining. The infarct size was significantly lower in the MSC coupled with NAC-transplanted group than in the naïve MSC-transplanted group (MSCs vs. MSCs–NAC: 15.8 ± 1.03 vs. 6.0 ± 0.88, respectively, $p < .05$) (Fig. 4B). The incidence of TUNEL-positive myocardial cells was significantly reduced in the MSC coupled with NAC-transplanted group compared to the MSC-only-transplanted group (MSCs vs. MSCs–NAC: 14.6 ± 1.2% vs. 8.4 ± 0.7%, respectively, $p < .01$) (Fig. 4C). The mean microvessel count per field in the infarcted myocardium was significantly higher in the MSC coupled with NAC-transplanted group than in the other group (MSCs vs. MSCs–NAC: 83 ± 14 vs. 127 ± 9, respectively, $p < .01$) (Fig. 4D). In addition, we observed that treatment of NAC had no effects on the infarct size, the number of apoptotic cells, and the microvessel density in our experimental conditions, indicating that the observed beneficial effects were due to enhanced survival and engraftment of MSCs by elimination of free radicals in transplanted environment, not directly by NAC (Fig. 4B–4D).

Discussion

Autologous MSCs offer a great advantage when used to generate functional cardiac myocytes because they can be easily prepared from adult patients and they are immunologically safe. However, the frequency of MSC engraftment is extremely low despite the implantation of large numbers of cells due to a low rate of cell adhesion and survival [24]. Despite the numerous approaches that have been attempted to overcome these limitations and dramatically improve cardiac function in a rodent MI model, there is still no solution to the

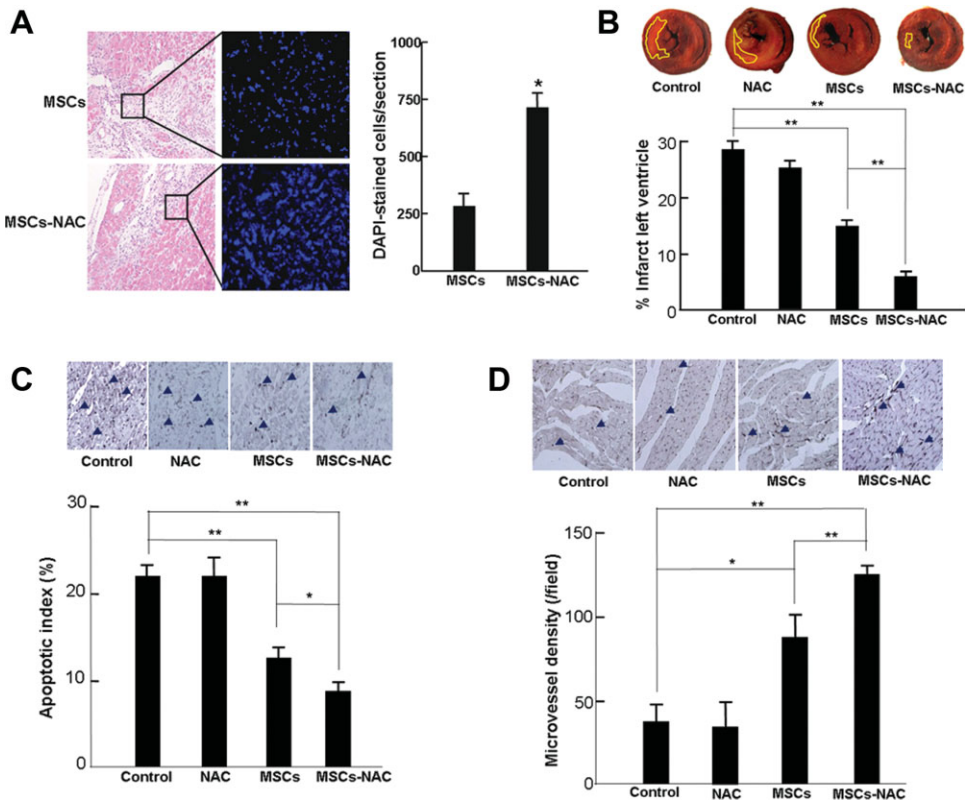

Figure 4. Changes in representative histological sections after implantation of MSCs coupled with NAC. **(A):** Detection of viable MSCs in ligated hearts by co-injection with NAC. Three days after implantation of DAPI-labeled MSCs into a myocardial infarction (MI)-induced animal, DAPI-labeled cells were observed by fluorescence microscopy. **(B):** Intramyocardial co-injection of MSCs with NAC reduced the left ventricular infarct size as assessed by 2,3,5-triphenyltetrazolium chloride staining at seven days post-MI. **(C):** Apoptosis assay on heart tissue, one week after left anterior descending (LAD) ligation. The left panel shows representative transferase-mediated dUTP nick-end labeling staining images (magnification: 200×). Staining for normal nuclei (green) was conducted using methyl green, and apoptotic nuclei are brown. **(D):** Quantitative analysis for evaluating microvessel density was conducted. Values are the average of three measurements with the S.D. indicated by error bars (*, $p < .05$, **, $p < .01$). Abbreviations: DAPI, 4′,6-diamidino-2-phenylindole; MSCs, mesenchymal stem cells; NAC, *N*-acetyl-L-cysteine.

problem of anoikis, programmed cell death induced by loss of matrix attachments [8]. Indeed, engrafted MSCs first encounter harsh conditions coupled with the loss of survival signals because of an inadequate interaction between cells and matrix [9]. Because substantial amounts of ROS are generated in the high-risk area in ischemia/reperfusion-injured hearts and because ROS is known to affect cell adhesion, we investigated the effects of ROS on adhesion, spreading, and cellular signaling of MSCs.

On the basis of our observations, exogenous ROS significantly impaired adhesion and spreading of MSCs. However, scavenging ROS from NAC treatment successfully restored the altered adhesion and spreading of MSCs, indicating that hindered adhesion and spreading of MSCs are ROS-specific. In addition, we observed that the expression levels of integrin molecules, such as αV and β1, and the phosphorylation of focal adhesion kinases, such as FAK and Src, were significantly decreased in exogenous ROS-treated MSCs but were rescued by NAC, suggesting that ROS-mediated loss of cell–matrix adhesion is associated with an integrin-dependent pathway. In fact, integrins are essential for cell migration and invasion because they mediate the adhesion of cells to the extracellular matrix and regulate intracellular signaling pathways that control cytoskeletal organization, force generation, and survival [25]. Focal adhesions are integrin-based structures that mediate strong cell–substrate adhesion and transmit information in a bidirectional manner between extracellular molecules and the cytoplasm [26–28]. Activated integrins bind to the extracellular matrix, cluster at the binding site, and initiate focal adhesions by recruiting cytoplasmic proteins, such as focal adhesion kinase (FAK), Src, and paxillin [21]. Our finding that the expression level of Rac-1 was significantly decreased in exogenous ROS-treated MSCs is consistent with the report that integrins activate Rac-1, which in turn activates downstream effector molecules, leading to the rearrangement of actin stress fibers and activation of cell adhesion and spreading [23]. Furthermore, we observed a similar pattern in the loss of adhesion in ROS-treated MSCs on cardiogel, indicating that ROS may hinder the adhesion of transplanted MSCs in biological circumstances because cardiogel is a 3D matrix that mimics the biological environment of the region into which the cells are injected. Immunocytochemical staining for integrin molecules further showed that ROS disrupted colocalization between integrin β1 and p-FAK in MSCs and downregulated the expressions of integrin β1 and p-FAK. The distribution of focal adhesion-related proteins such as paxillin, vinculin, and talin were also disrupted, suggesting that ROS generated in an infarcted area might be a major obstacle to adhesion and survival of engrafted MSCs for cardiac repair.

According to our in vivo histological findings, three times more transplanted MSCs–NAC were retained in the border region than naïve MSCs. In addition, transplantation of MSCs–NAC resulted in a further decrease in infarct size and improvement of microvessel density compared to transplantation with MSCs in the absence of NAC. Since improvement in cardiac structure is related to a reduction in infarct size and a higher capillary density, MSCs–NAC may mediate an increase in microvessel formation that increases blood flow within the infarcted area and contributes to inhibition of cardiac remodeling and subsequent improvement in systolic function. These histological parameters show that scavenging ROS coupled with MSC transplantation improves the cardiac regenerative capacity of MSCs.

Conclusion

In this report, we demonstrated that ROS, a major cause of injury after ischemia/reperfusion, may hinder the adhesion and spreading of MSCs, and scavenging ROS successfully improves the adhesiveness of engrafted MSCs in the infarcted heart, leading to beneficial effects for cardiac repair. In addition, it was revealed that the loss of adhesion of MSCs by ROS is dependent on the integrin-related focal adhesion pathway. Our finding that co-injection of MSCs with antioxidant enhances the viability and integration potential of MSCs may provide novel therapeutic opportunities for the treatment of myocardial infarction and end-stage cardiac failure. In future studies, dissecting the mechanism of action of adhesion-related molecules might have important implications for the development of engrafted stem cell therapy for cardiac repair in ischemic-injured hearts.

Acknowledgments

This research was supported by a Korea Science and Engineering Foundation (KOSEF) Grant funded by MOST (M1064102000106N410200110), a grant (SC-2150) from Stem Cell Research Center of 21st Century Frontier Research Program funded by the Ministry of Education, Science and Technology, Republic of Korea and by the Korea Science, and a grant from the Korea Health 21 R&D Project, Ministry of Health & Welfare, Republic of Korea (A085136).

Disclosure of Potential Conflicts of Interest

The authors indicate no potential conflicts of interest.

References

1 Lopez AD, Mathers CD, Ezzati M et al. Global and regional burden of disease and risk factors, 2001: Systematic analysis of population health data. Lancet 2006;367(9524):1747–1757.
2 Orlic D, Kajstura J, Chimenti S et al. Bone marrow cells regenerate infarcted myocardium. Nature 2001;410(6829):701–705.
3 Stamm C, Westphal B, Kleine HD et al. Autologous bone-marrow stem-cell transplantation for myocardial regeneration. Lancet 2003; 361(9351):45–46.
4 Wollert KC, Meyer GP, Lotz J et al. Intracoronary autologous bone-marrow cell transfer after myocardial infarction: The BOOST randomized controlled clinical trial. Lancet 2004;364:141–148.
5 Hahn JY, Cho HJ, Kang HJ et al. Pre-treatment of mesenchymal stem cells with a combination of growth factors enhances gap junction formation, cytoprotective effect on cardiomyocytes, and therapeutic efficacy for myocardial infarction. J Am Coll Cardiol 2008;51:933–943.
6 Mangi AA, Noiseux N, Kong D et al. Mesenchymal stem cells modified with Akt prevent remodeling and restore performance of infarcted hearts. Nat Med 2003;9:1195–1201.
7 Li W, Ma N, Ong LL et al. Bcl-2 engineered MSCs inhibited apoptosis and improved heart function. Stem Cells 2007;25:2118–2127.
8 Ingber DE. Mechanical signaling and the cellular response to extracellular matrix in angiogenesis and cardiovascular physiology. Circ Res 2002;91:877–887.
9 Mylotte LA, Duffy AM, Murphy M et al. Metabolic flexibility permits mesenchymal stem cell survival in an ischemic environment. Stem Cells 2008;26:1325–1336.

10 Oshima Y, Fujio Y, Nakanishi T et al. STAT3 mediates cardioprotection against ischemia/reperfusion injury through metallothionein induction in the heart. Cardiovasc Res 2005;65:428–435.
11 Angelos MG, Kutala VK, Torres CA et al. Hypoxic reperfusion of the ischemic heart and oxygen radical generation. Am J Physiol Heart Circ Physiol 2006;290:H341–H347.
12 Yao EH, Yu Y, Fukuda N. Oxidative stress on progenitor and stem cells in cardiovascular diseases. Curr Pharm Biotechnol 2006;7: 101–108.
13 Chiarugi P, Buricchi F. Protein tyrosine phosphorylation and reversible oxidation: Two cross-talking posttranslation modifications. Antioxid Redox Signal 2007;9:1–24.
14 Pelegrin P, Surprenant A. Dynamics of macrophage polarization reveal new mechanism to inhibit IL-1beta release through pyrophosphates. EMBO J 2009;28:2114–2127.
15 Chang W, Song B-W, Lim S et al. Mesenchymal stem cells pretreated with delivered Hph-1-Hsp70 protein are protected from hypoxia-mediated cell death and rescue heart functions from myocardial injury. Stem Cells 2009;27(9):2283–2292.
16 Song S-W, Chang W, Song B-W et al. Integrin-linked kinase is required in hypoxic mesenchymal stem cells for strengthening cell adhesion to ischemic myocardium. Stem Cells 2009;27(6):1358–1365.
17 Zvibel I, Smets F, Soriano H. Anoikis: Roadblock to cell transplantation. Cell Transplant 2002;11:621–630.
18 Akimov SS, Krylov D, Fleischman LF et al. Tissue transglutaminase is an integrin-binding adhesion coreceptor for fibronectin. J Cell Biol 2000;148:825–838.
19 Cukierman E, Pankov R, Stevens DR. Taking cell-matrix adhesions to the third dimension. Science 2001;294:1708–1712.
20 Thomas FT, Contreras JL, Bilbao G et al. Anoikis, extracellular matrix, and apoptosis factors in isolated cell transplantation. Surgery 1999;126:299–304.
21 Hui AY, Meens JA, Schick C et al. Src and FAK mediate cell-matrix adhesion-dependent activation of Met during transformation of breast epithelial cells. J Cell Biochem 2009;107(6):1168–1181.
22 Salsmann A, Schaffner-Reckinger E, Kabile F et al. A new functional role of the fibrinogen RGD motif as the molecular switch that selectively triggers integrin aIIbh3-dependent RhoA activation during cell spreading. J Biol Chem 2005;280:33610–33619.
23 Liu S, Kapoor M, Leask A. Rac1 Expression by Fibroblasts Is Required for Tissue Repair *in Vivo*. Am J Pathol 2009;174(5): 1847–1856.
24 Watanabe E, Smith DM Jr., Delcarpio JB et al. Cardiomyocyte transplantation in a porcine myocardial infarction model. Cell Transplant 1998;7:239–246.
25 Ames BN, Shigenaga MK, Hagen TM. Oxidants, antioxidants, and the degenerative diseases of aging. Proc Natl Acad Sci U S A 1993;90: 7915–7922.
26 Yamada KM, Geiger B. Molecular interactions in cell adhesion complexes. Curr Opin Cell Biol 1997;9(1):76–85.
27 Hynes RO. Integrin: Versatility, modulation and signaling in cell adhesion. Cell 1992;69:11–25.
28 Schwartz MA, Schaller MD, Ginsberg MH. Integrins: Emerging paradigms of signal transduction. Annu Rev Cell Dev Biol 1995;11:549–599.

See www.StemCells.com for supporting information available online.